

Identification of Micro-scale Defects in Crystalline Solar Cell Structure

Jiri Sicner^{1*}, Pavel Koktavy¹, Dinara Dallaeva¹

¹ Brno University of Technology, Faculty of Electrical
Engineering and Communication, Department of Physics
Technicka 8, 616 00 Brno
Czech Republic
xsicne02@stud.feeec.vutbr.cz

Keywords: Solar cell, local defect, fractured surface, nondestructive testing.

Abstract

The article deals with the diagnostics application to local defects on the edge in silicon solar cells by monitoring their optical and thermal activities during electrical excitation. During the measurement is solar cell connected to a voltage source in the reverse direction. Radiation generated from reverse-biased *pn* junction defects is used to study local properties. It proves to be useful to measure surface radiation and to make light spots (defects) localization. By the same way is possible to measure the radiation intensity. We also focused on thermal degradation in stressed regions. To this aim we used an infrared camera and it turns out that temperature degradation could occur in large scale region compare to micro-scale defects.

Introduction

Silicon monocrystalline ingots are used as a source material during the production of solar cells. These ingots are cutted to wafers by a diamond wire. Square substrats from round wafers are prepared by the diamond saw precutting and by following breaks. In course of this process micro-scale defects and inhomogenities occurred at the edges. Subsequently these defects significantly reduce the efficiency and reliability of the solar cells.

Generally, devices based on *pn* junction are tested using electric measurement, luminescence techniques and laser beam induced current techniques. For example luminescence and beam induced techniques are widely used for defects localization. Some of these defects can be localized in microscale region using scanning probe microscope [1]. Although imperfections are small about micrometer they affect behavior of the whole solar cell samples [2]. For the defect classification purposes it is useful to measure its light emission thermal dependence while the sample is in reverse-biased conditions [3].

This article deals with local defects (fractures) on edges of silicon solar cells. We observed a certain type of structure defects (see Fig. 1) by an electron microscope which could be assume as surface texturization break. Specimens including this type of local defects have been put under investigation. We put forward results of novel noise diagnostics and optical characterization. We study weak radiation generated from reverse-biased defect active area by means of a photomultiplier and a scientific CCD camera. This approach proves to be useful to measure micro-scale surface imperfections and fractures. Important results are related to non-existence of defects creating massive conductive channel in geometrically similar form located in the bulk. Nevertheless, mass-produced crystalline material exhibits this type of defects very often.

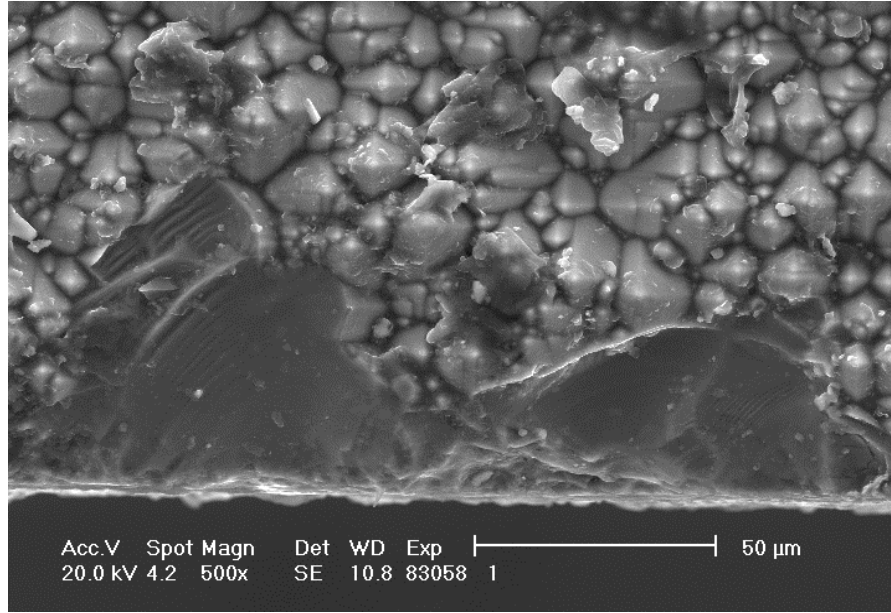


Fig. 1. Detail of damaged surface structure on the edge of silicon solar cell (specimen K22)

Solar cells under investigation in detail

Primary solar cells what we use are made of mono-crystal silicon, of dimensions (10×10) cm and a thickness of about $230 \mu\text{m}$. The *p* and *n* layers (bottom and top-side, respectively) are formed by diffusion. The *p* type substrate is made by the Czochralsky process with the resistivity of about $1.2 \Omega\text{cm}$. The upper face of the cell is geometrically textured by pyramids to reduce the light reflection. A silicon nitride layer, which is laid on the cell surface, is intended to passivate the silicon surface and again reduces the reflection losses. The cells are designed for the solar panel fabrication. Both complete cells and their broken fragments have been studied but only selected results are presented here. The screen-printed silver paste metallization was used for contacts on the front side. The back side of solar cells has a structure of Al BSF with Ag/Al busbars. The *pn* junction is localized close to the surface and traces pyramidal texturization. The depletion layer width is about of $0.6 \mu\text{m}$ (without the applied bias voltage) [4].

Experimental details

Optical characteristics in visible range. Radiation generated from reverse-biased *pn* junction defects or their neighborhood is used to study the near field or far field local properties. It proves to be useful to measure surface radiation and to make light spots localization, to measure the radiation intensity versus voltage plot, its correlation with other, mainly noise characteristics and radiation spectrum. A scientific CCD camera G2-3200 with a 3.2 MPx resolution was used for measuring of the radiation from a *pn* junction solar cell surface in optical far field. It uses a silicon chip cooled by dual system of Peltier's modules with the temperature down to -50°C . Sufficient temperature for normal working mode is of -10°C . The Dark current of an optical sensor and a single pixel is 0.8 e/s ($T = 0^\circ\text{C}$) and the doubling of its value is reached for a temperature rise of 6°C . The dynamic range of the elementary pixels with a usable range up to 16 bits is very good. A camera lens with the focal ratio of 1.2 and the working aperture of 41.7 mm is used with the camera. It is possible to measure in the useful range of wavelengths of 300 nm – 1100 nm. Since the producer defines the spectral characteristics of the particular CCD chip, photometry measurements can be performed as in our case. The mean quantum efficiency $\langle\text{QE}\rangle = 0.51$ is reached in the interval from 300 nm to 1100 nm. The peak value of the quantum efficiency is of 0.82 at the wavelength of 647 nm. Optical filters are included to an optical path to obtain the spectral characteristics. Automatic carousel system is equipped with filters to watch

for visible and infrared radiation and in addition with interval filters separating the visible part of spectrum into red, green and blue parts. FWHM (Full Width at Half Maximum) of the filters are 150 nm and their optical response is calibrated. It is possible to include interference filters with FWHM of about 10 nm ahead of the lens. Detected radiation is relatively weak due to their high selectivity and this measurement is very technically and time demanding. The calibration is not performed separately for each of these filters, but measurement is carried out with the average spectral transmission function. The results are therefore correct in principle but we work with them in relative terms [5].

Thermal characteristics. For measurement of thermal characteristics the infrared camera (Micro-Epsilon TIM 160 Infrared Process Imager) was used. The 160x120-pixel detector and high-performance optics guarantee precise temperature measurements of target objects as small as 1.5 mm (3 pixels) at a measuring rate of 120 Hz. The IR camera has wide temperature range from -20°C to 900°C and spectral range from 7.5 to 13 μm. Thermal sensitivity is very good and starts from 80 mK.

Results

Presented research is focused on the defects localized on the edges of solar cells. Existing knowledge indicates that areas on the edges or near them are responsible for huge breakdowns, [6], [7]. This interpretation is supported by measurement of specimen X2 as presented below (see characteristics on fig. 2a and photography on fig. 2b).

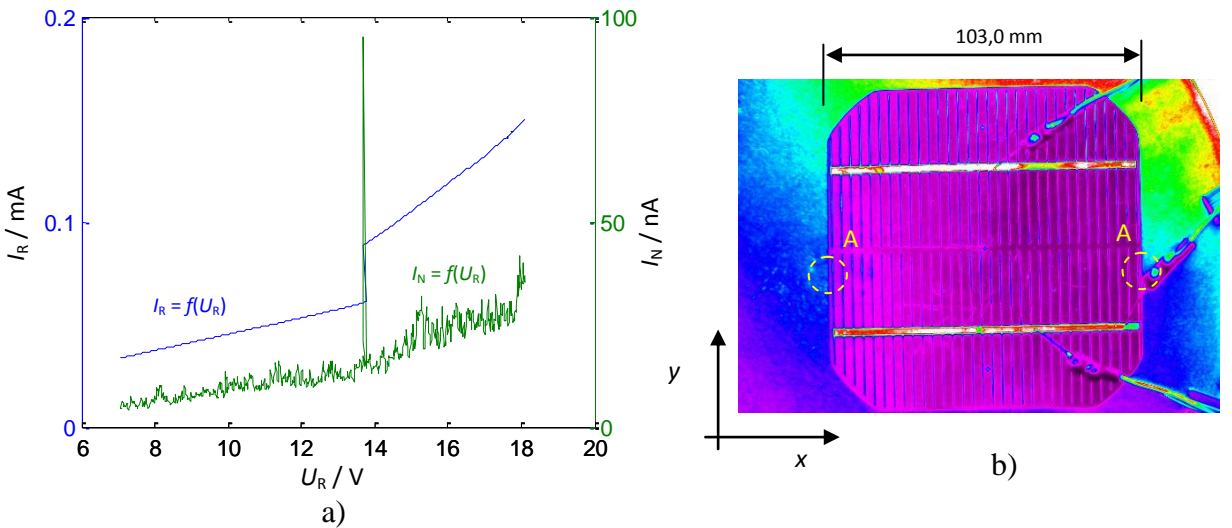


Fig. 2. a) Narrowband noise signal and the reverse current dependence on applied reverse voltage U_R . Sample X2 at temperature $T = 24.3$ °C. b) Photo of solar cell X2 taken by a CCD camera with light bias

The measurement clearly shows that after reaching a critical voltage there are two defects, both on the edges (see fig. 3), and it is not obviously clear which of them dominantly contributes to the shape of characteristic. Nevertheless, important results are related to non-existence of bulk defects creating massive conductive channel [8]. In additional, in course of another measurement has not been found similar defects located close to the break-like edges. It means that the studied edges that were created by control breaking solar cell seems to be much better quality than edges which are subjected to passivation process in production. Suggested results indicate that passivated edges by producer are not processed properly.

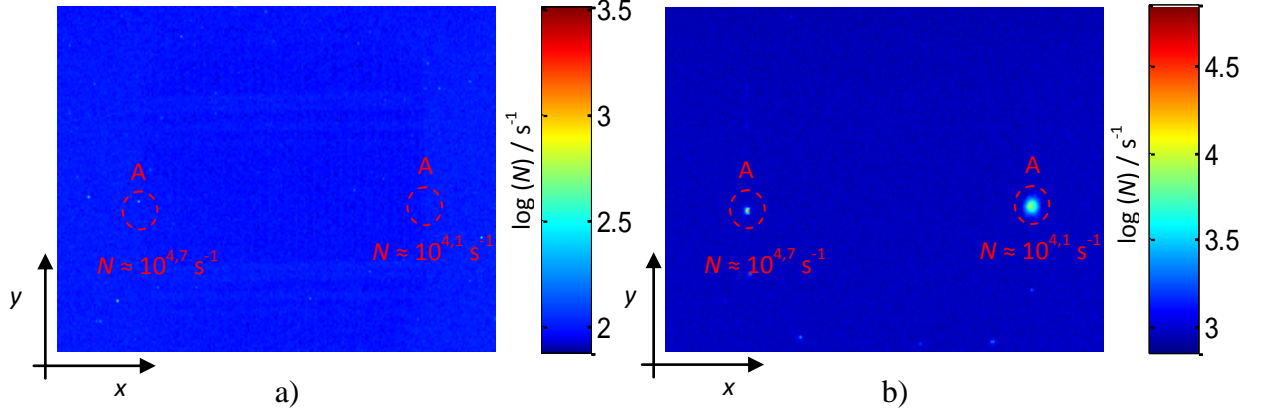


Fig. 3. a) State of photon emission before reaching the critical voltage ($U_R = 11$ V), b) after the breakdown ($U_R = 16$ V), $T = 24.3$ °C

This suggestion was supported by measurement of sample K20 (see fig. 4), where local defect at the boundary was found. Next we use again the CCD camera with a special lens and an electron microscope to study minute details of the defect. As can be seen from the detail in the Fig. 4, the defective area is located on the border between surface and edge of solar cell i.e. the *pn* junction region. This fact can be very dangerous for lifetime of a solar cell.



Fig. 4. Detail of light emission from defect on the edge. Sample K20 taken by CCD camera with light bias.

Figure 5 represents I–V characteristics and light emissions vs. reverse bias measured on the observed imperfections from sample K22 (see fig. 7). The light emission from these observed imperfections depends on reverse voltage. There we can see two local micro-sized defects on the edge of solar cell and according to the radiation characteristics. It is clear that each of them have the same origin. As is shown in fig. 5, defect labeled as a “spot 1” starts to radiate at reverse voltage about 4,8 V whereas the defect labeled as “spot 2” starts to radiate at reverse voltage about 5 V. Processes which are occurred after reaching critical voltage can be described by noise characteristic [9], [10]. Characteristics of these spots are a typical for defects on the edge of solar cells which are caused by damage surface texturization.

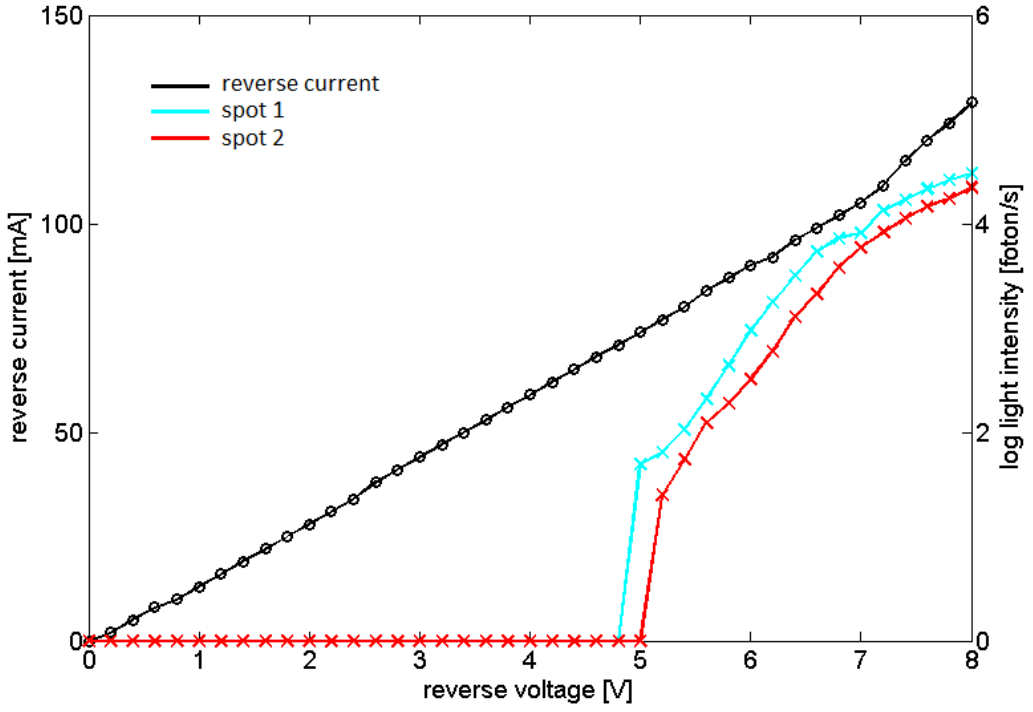


Fig. 5. Reverse current and light emission dependence on reverse-bias voltage measured on sample K22.

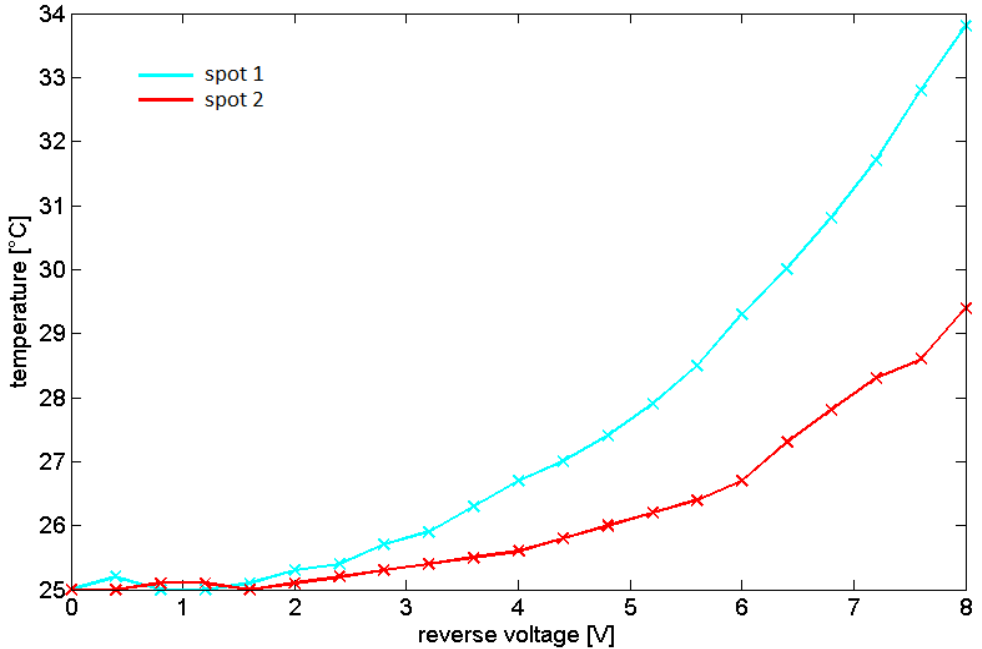


Fig. 6. Temperature dependence of spot 1 and 2 on the reverse voltage, K22, IR camera.

As shown in Fig. 7, a sample K22 contains two significant local defects. It managed to show that the thermal radiation can be seen that the thermal degradation causes both defects on the edge (see Fig. 8). When the sample is connected to a reverse voltage 6V, the temperature at the defect “spot 1“ on the edge increased by 4 °C and we can see that the temperature of defect area increases rapidly at higher voltages (see Fig. 6). It is clear that at higher voltages may occur complete destruction of the sample.

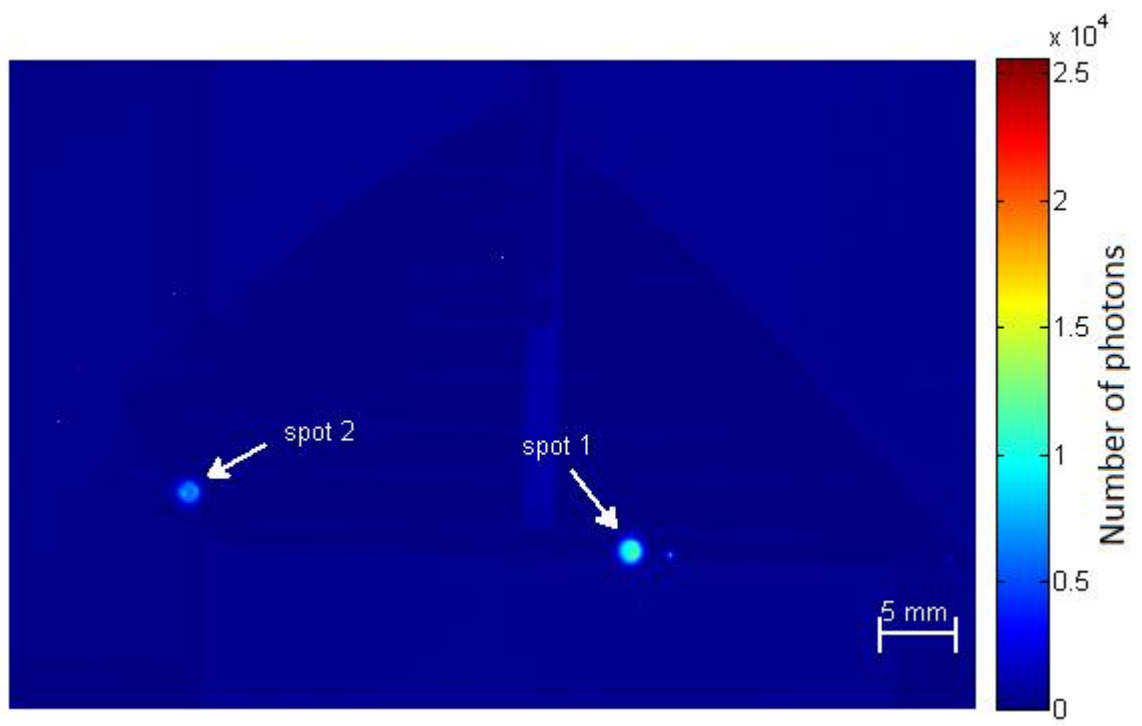


Fig. 7. Photography of measured solar cell with light spots and their intensity, sample K22, reverse voltage 6 V, CCD camera was used.

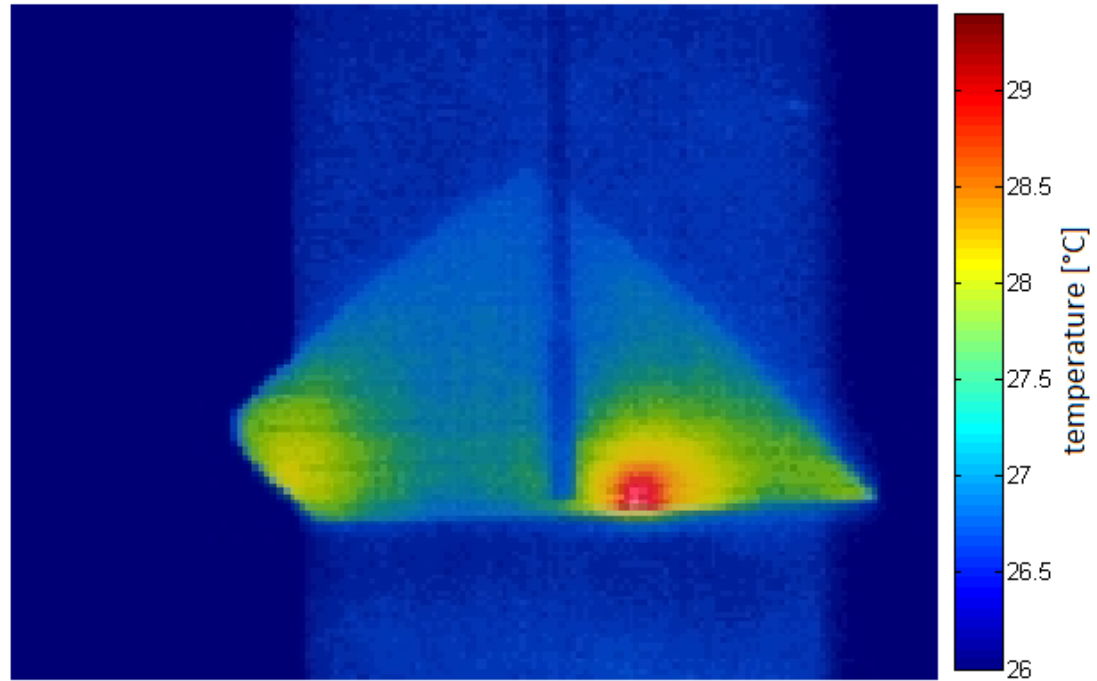


Fig. 8. Surface temperature distribution, thermal flux induced by defect on the edge, sample K22, reverse voltage 6 V.

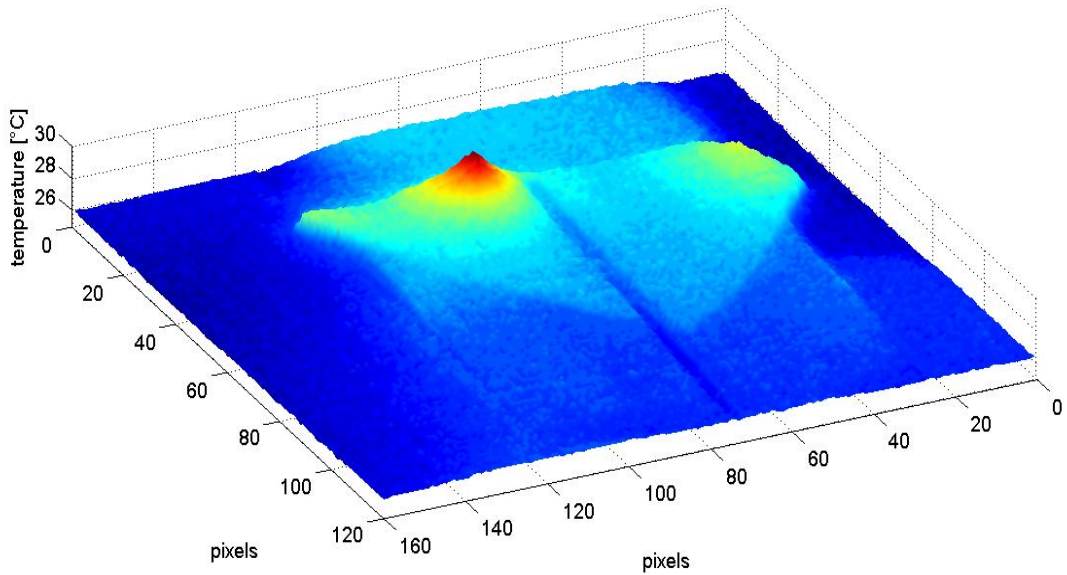


Fig. 9. Surface temperature distribution in 3D, thermal flux induced by defect on the edge, sample K22, reverse voltage 6 V, 10 pixel ~ 8mm.

Summary

We can conclude that light and thermal emission from a reverse biased solar cell can reveal structure inhomogeneities. Many defects exhibit radiation from a surface of solar cells. It proves to be useful to measure this radiation by means of the CCD camera. We focused on defects on the edge of solar cells in this paper. As we have shown, this type of defect can be very dangerous for efficiency and service life of a solar cell. This approach proves to be useful to measure micro-scale surface imperfections and fractures. Important results are related to non-existence of defects creating massive conductive channels in geometrically similar form located in the bulk. Nevertheless, mass-produced crystalline material exhibits this type of defects very often. This points to the fact that the process of passivation of edges of solar cells is not ideal. An interesting fact is that the edges that are created by breaking of solar cells does not contain this type of defect. We are currently working on isolation of edges with laser notches in their neighbourhood. Laser notch will be realized deep compared to the PN junction thickness and they represent defined insulating structure. It should be noted that the melting or solidification of the material is strictly necessary to optimize because there are arising relatively conductive amorphous structure.

Acknowledgement

This paper is based on the research supported by the Grant Agency of the Czech Republic, the grant No. P102/10/2013, on the research supported by the Ministry of Industry and Trade of the Czech Republic, the project MPO TIP FR-TI1/305, on the research supported by the Grant Agency of the Czech Republic within the framework of projects GACR 102/09/H074 "Diagnostics of material defects using the latest defectoscopic methods" and on the SIX research centre (project registration number: CZ.1.05/2.1.00/03.0072).

References

- [1] P. Skarvada, P. Tomanek, L. Grmela and S. Smith: Sol. Energ. Mat. Sol. C., Vol. 94 (2010), p. 2358-2361.
- [2] P. Skarvada, L. Grmela, P. Tomanek: Key Eng. Mat., Vol. 465 (2011), p. 239-242.
- [3] L. Grmela, P. Skarvada, P. Tomanek, R. Macku, S. Smith: Sol. Energ. Mat. Sol. C., Vol. 96 (2012), p. 108-111.
- [4] P. Koktavy, R. Macku: 21st International Conference on Noise and Fluctuations, (2011).
- [5] R. Macku: EEICT, Vol. 3 (2011), p. 417-421.
- [6] A. G. Chynoweth, K.G. McKay: Phys. Rev, vol. 102 (1956), p. 369 – 376.
- [7] P. Skarvada, P. Tomanek, P. Koktavy, R. Macku: 9th International Conference on Environment and Electrical Engineering, (2010).
- [8] P. Paracka, P. Koktavy, O. Krcal: Non-destructive testing in engineering practice, (2007).
- [9] R. Macku, P. Koktavy: Physica status solidi, Vol. 207 (2010), p. 2387-2394.
- [10] P. Koktavy, J. Vanek, Z. Chobola, K. Jandova, J. Kazelle: Proceeding of AIP, (2007).